

*Type of contribution:* **Paper**

## **Deposition of boehmite on carbon nanofibers using aluminum alkoxide and its thermal transformation**

**Seiichi Taruta, \* Ayaka Suzuki, Yoshio Arai, Naoki Ueda,  
Tomohiko Yamakami and Tomohiro Yamaguchi**

**Department of Chemistry and Materials Engineering, Faculty of Engineering,  
Shinshu University,**

4-17-1 Wakasato, Nagano-shi, Nagano 380-8553, Japan

**\*Corresponding author:**

**Seiichi TARUTA**

**Department of Chemistry and Materials Engineering, Faculty of Engineering,  
Shinshu University, 4-17-1 Wakasato, Nagano-shi, Nagano 380-8553, Japan**

**TEL: +81-26-269-5416**

**FAX: +81-26-269-5424**

**E-mail: staruta@shinshu-u.ac.jp**

## **Abstract**

We attempted to prepare carbon nanofibers (CNFs) bonded chemically with alumina particles using acid-treated CNFs and aluminum sec-butoxide. The structure and morphology of the boehmite deposited on the CNFs, the boundary between the CNFs and the deposited boehmite, and the thermal transformation of the deposited boehmite were investigated using Raman spectroscopy, X-ray diffraction (XRD) analysis, field-emission scanning electron microscopy (FE-SEM), and transmission electron microscopy (TEM). The boehmite deposited not only particulate on the CNFs but also in a film-like manner on parts of the CNFs. In addition, the boehmite could deposit not only on the disordered inner walls of the CNFs but also on the ordered inner walls. By heating at 1200°C, the boehmite on the CNFs was transformed into  $\alpha$ -alumina and  $\theta$ -alumina. At this time, some alumina particles, particularly those formed on the ordered inner walls of CNFs, fell out of the CNFs, and only those alumina particles which might chemically bond with CNFs remained on the CNFs. Finally, CNFs dotted with alumina particles with a size of < 50 nm were obtained.

**Key words:** Sol-gel processes; Nanocomposites; Alumina; Carbon nanotube

## 1. Introduction

Carbon nanotubes (CNTs) have not only a high aspect ratio but also incredible mechanical properties, such as high tensile strength and high elasticity [1-8], so CNTs are regarded as attractive candidates for the reinforcement of ceramic materials. Many studies have reported on ceramics combined with CNTs, for example CNT/Al<sub>2</sub>O<sub>3</sub>, CNT/ZrO<sub>2</sub>, CNT/Si<sub>3</sub>N<sub>4</sub> and CNT/SiC composites, and so on. However, significantly higher performance based on CNTs has not always been obtained.

In our previous papers [9-11], we reported on combined alumina ceramics with carbon nanofibers (CNFs), which were a type of multi-walled carbon nanotube, and we have shown that the fracture toughness of the obtained CNF/alumina composites increased with a decrease in the average alumina grain size of the composites. This improvement was caused by the bridging and/or pull-out of bent CNFs along the alumina grain boundaries. In other words, straight CNFs in the composites almost did not perform the reinforcement, because hydrophobic CNFs were very easily pulled out from hydrophilic alumina matrices. Therefore, if a strong chemical bond is formed between CNFs and alumina matrices, even such straight CNFs will contribute to the improvement of fracture toughness. Such chemical bonding may be realized by combining alumina ceramics with CNFs, the surfaces of which are coated with alumina by chemical bonding.

There have been some reports on the alumina coating of CNTs. Hernadi et al.

prepared alumina, titania and silica coatings on CNTs using organometallic compounds as raw materials, and a homogenous alumina coating, accompanied by needle crystals, was obtained on CNTs using aluminum isopropoxide and no solvent [12]. They also reported that a homogenous amorphous alumina coating was prepared on CNTs with adsorbed sodium dodecyl sulfate as surfactant, using aluminum trichloride in 2-propanol [13]. Yang et al. reported that a continuous alumina coating, which was a  $\gamma$ -Al<sub>2</sub>O<sub>3</sub> layer with a thickness of 1-3 nm, was successfully prepared on CNTs modified with polyvinyl alcohol [14]. However, the boundaries and bonding between the coating and the CNTs have not been observed in detail, and the thermal transformation of the coating has not been investigated.

Therefore, in this study, we tried to prepare CNFs chemically bonded with alumina particles using acid-treated CNFs and aluminum sec-butoxide. We believed that chemical bonding between CNFs and alumina would be achieved through a dehydration reaction between the hydrophilic functional groups, such as the carboxylic (-COOH) and hydroxyl (-OH) groups, formed on the CNFs by acid-treating the CNFs and the alumina precursors formed by the hydrolysis of aluminum sec-butoxide. The structure and morphology of the alumina precursors deposited on the CNFs, the boundary between the CNFs and the deposited alumina precursors, and the thermal transformation of the alumina precursors were investigated.

## 2. Experimental procedure

The CNFs (VGCF-S; diameter: 100 nm, length: 10–20  $\mu\text{m}$ ; Showa Denko, Japan) used in this study were first soaked in an acid mixture (conc.  $\text{H}_2\text{SO}_4$ :conc.  $\text{HNO}_3 = 3:1$  v/v) for 0.5 and 5 h under ultrasonic conditions. The acid-treated CNFs were separated from the acid mixture by filtration, rinsed with distilled water, and then freeze-dried. In this paper, the CNFs soaked in the acid mixture for 0.5 and 5 h are described as AT05-CNFs and AT5-CNFs, respectively.

Under ultrasonic conditions, 0.05 g of AT05-CNFs or AT5-CNFs was dispersed in 200 mL of water. The obtained AT05-CNF and AT5-CNF suspensions were then heated to 100°C and 0.05 g of aluminum sec-butoxide was added to them. These suspensions were refluxed at 100°C for 18 h, cooled to room temperature, and then kept still for 3 days to sediment the CNF bundles, CNF agglomerates, and large alumina precursors into the bottom layer of the suspensions. Then, these suspensions were elutriated; namely, only the upper layers of these suspensions, where the CNFs would be well dispersed, were extracted from these suspensions. The extracted upper layers were filtered, and the separated AT05-CNFs and AT5-CNFs were rinsed with distilled water and freeze-dried. Alumina precursor was deposited on the separated and rinsed AT05-CNFs and AT5-CNFs. And these AT05-CNFs and AT5-CNFs are described as alumina precursor-deposited AT05-CNFs and AT5-CNFs, respectively. Finally, they were heated at 1200°C for 1 h under vacuum.

The prepared specimens were evaluated using Raman spectroscopy, X-ray diffraction (XRD) analysis, field-emission scanning electron microscopy (FE-SEM), and transmission electron microscopy (TEM).

### 3. Results

#### 3.1 Acid-treated CNFs

The Raman spectra of the acid-treated CNFs were reported in our previous paper [10]. According to the results, the intensity ratio of the D-band (defect-mode) to the G-band ( $E_{2g2}$  mode) increased with the acid-treatment time. That is, defects were induced on the CNFs by acid treatment and increased with the acid-treatment time. The TEM images of pristine CNFs and AT5-CNFs are shown in **Fig. 1**. The pristine CNFs had smooth surfaces and their inner walls were ordered at even intervals. On the other hand, the AT5-CNFs had rough surfaces and their inner walls were disordered. In addition, the defects, like depressions, were formed on the surface of the AT5-CNFs, as shown by circles in Fig. 1 (d). Similar defects were observed by Yamamoto et al. [15]. So the acid-treated CNFs, especially AT5-CNFs, were dispersed uniformly in water under ultrasonic conditions, but the pristine CNFs were not. The above results mean that the surfaces of the acid-treated CNFs were modified with hydrophilic functional groups, such as carboxylic (-COOH) and hydroxyl (-OH) groups [16,17].

#### 3.2 Deposition of boehmite on CNFs

The XRD patterns of the alumina precursor-deposited AT05-CNFs and AT5-CNFs are shown in **Fig. 2**. These patterns indicate that boehmite was formed by the hydrolysis of aluminum sec-butoxide and the dehydration condensation reactions in both specimens.

After this, the alumina precursor-deposited AT05-CNFs and AT5-CNFs are described as boehmite-deposited AT05-CNFs and AT5-CNFs, respectively.

The FE-SEM images of the boehmite-deposited AT05-CNFs and AT5-CNFs are shown in **Fig. 3**. The boehmite deposited as particles on both AT05-CNFs and AT5-CNFs. Also, such particulate boehmite was scattered uniformly on these CNFs. Besides, boehmite particles, which were not on these CNFs, and large boehmite agglomerates were formed in both AT05-CNF and AT5-CNF suspensions, which are not shown in this paper, and most of them were removed by elutriating these suspensions.

The TEM images of the boehmite-deposited AT05-CNFs and AT5-CNFs are shown in **Fig. 4**. The particulate boehmite with an irregular shape and non-uniform sizes deposited on the AT05-CNFs, and needle-like particles were also observed. The morphology of the formed boehmite was similar to that of alumina precursors formed on the CNTs using aluminum isopropoxide [12]. A special feature of the boehmite deposited on the AT5-CNFs was the large particle size of about 50 nm, as indicated by the arrows in Fig. 4 (c). Such boehmite particles were largely not observed on AT05-CNFs. The interfaces between such large boehmite particles and CNFs are shown in Fig. 4 (d) and (f). The preparation procedure of the boehmite shown in Fig. 4 (f) was slightly different from that mentioned in the experimental procedure in this paper. The point of difference was that the AT5-CNFs and aluminum sec-butoxide were added to the water at the same time, treated by ultrasound, and then refluxed at 100°C. These

images suggest that such boehmite particles were directly generated on the CNFs and grew, so they might chemically bond with CNFs. Because the AT5-CNFs had a larger amount of hydrophilic functional groups, such as carboxylic (-COOH) and hydroxyl (-OH) groups, as defects, many boehmite particles might chemically bond with carboxylic (-COOH) and hydroxyl (-OH) groups modified on the CNFs through the dehydration reaction. In addition, boehmite coatings with a thickness of < 20 nm, like a film, were formed on parts of the surface of AT5-CNFs, as shown in Fig. 4 (e), which were also observed on parts of the AT05-CNF surfaces, as well as on the ordered inner walls of both AT05-CNFs and AT5-CNFs.

### 3.3 Thermal transformation of boehmite on CNFs

The boehmite-deposited AT05-CNFs and AT5-CNFs were heated at 1200°C for 1 h under vacuum. The XRD patterns of the heated boehmite-deposited AT05-CNFs and AT5-CNFs are shown in **Fig. 5**. These patterns indicate that the boehmite on the AT05-CNFs and AT5-CNFs was transformed into  $\alpha$ -alumina and  $\theta$ -alumina at 1200°C. It is known that boehmite is transformed into  $\alpha$ -alumina at 1000-1100°C via transition aluminas, such as  $\gamma$ -,  $\delta$ -, and  $\theta$ -aluminas [18]. Transition aluminas, such as  $\theta$ -alumina that were transformed from boehmite on the CNFs at lower temperatures could not be completely transformed into  $\alpha$ -alumina by heating at 1200°C for 1 h under vacuum. After this, the boehmite-deposited AT05-CNFs and AT5-CNFs that were heated at

1200°C for 1 h under vacuum are described as alumina-deposited AT05-CNFs and AT5-CNFs, respectively.

Shown in **Fig. 6** are the FE-SEM images of the alumina-deposited AT05-CNFs and AT5-CNFs. Comparing those images with those in Fig. 3, it is clear that the amount of deposition on the AT05-CNFs and AT5-CNFs was decreased by heating. This decrease resulted from a phase transformation together with volume shrinkage. That is, the transformation from boehmite with a smaller theoretical density ( $3.134 \text{ g/cm}^3$ ) to transition aluminas and  $\alpha$ -alumina with larger theoretical densities ( $\theta$ -alumina:  $3.616 \text{ g/cm}^3$ ,  $\alpha$ -alumina:  $3.987 \text{ g/cm}^3$ ) caused volume shrinkage. Through shrinkage, some alumina particles fell out of these CNFs. As a result, the AT05-CNFs and AT5-CNFs were dotted with alumina particles  $< 50 \text{ nm}$ . Among the depositions, a few hexagonal platelet particles were observed, as shown by arrows, which were euohedral of  $\alpha$ -alumina crystal. Their sizes were about  $100 \text{ nm}$  and were larger than the boehmite particles, which means that the depositions on the CNFs grew during their thermal transformation.

The TEM images of the alumina-deposited AT05-CNFs and AT5-CNFs are shown in **Fig. 7**. These images show the interfaces between the alumina particles ( $\alpha$ - or  $\theta$ -alumina) and CNFs, which indicates that the alumina particles tightly adhered to the CNFs. These interfaces were not always clear and other phases were not observed there. In addition, the disordered inner walls of the CNFs were observed near the non-clear

interfaces. These results suggest that the alumina particles might chemically bond with the CNF surfaces on which many defects are induced.

The Raman spectra of AT05-CNFs, boehmite-deposited AT05-CNFs, and alumina-formed AT05-CNFs are shown in **Fig. 8**. The D- and G-bands were observed at  $1315\text{ cm}^{-1}$  and  $1582\text{ cm}^{-1}$ , respectively. The intensity ratio of the D-band to the G-band (D/G ratio) for the AT05-CNFs was 0.43. And the D/G ratios of the three specimens were almost the same (0.40-0.48), which indicates that defects were almost not induced on AT05-CNFs by the formation of boehmite on the CNFs and by the transformation of the boehmite during heating at  $1200^{\circ}\text{C}$  under vacuum.

#### 4. Discussion

In this study, CNFs that might chemically bond with alumina particles ( $\alpha$ - or  $\theta$ -alumina) were finally obtained. The formation processes are shown in **Fig. 9**. Aluminum sec-butoxide was used as the starting material for alumina in this study. It was hydrolyzed immediately to form boehmite precursors when adding to heated water. Among the formed boehmite precursors, the dehydration condensation reactions caused the formations of boehmite sols in the solution. As shown in Fig. 9 (a), the boehmite precursors also directly caused dehydration reactions with hydrophilic functional groups, such as carboxylic (-COOH) and hydroxyl (-OH) groups, modified on the CNFs. Furthermore, dehydration reactions were also created between the boehmite sols formed in the solution and the hydrophilic functional groups on CNFs. If these dehydration reactions actually occur, chemical bonding forms between the boehmite and CNF. Next, the boehmite sols and boehmite precursors on the CNFs reacted with boehmite sols in the solution. These were dehydration condensation reactions and were produced again and again between the boehmite formed on the CNFs and the boehmite sols in the solution, as shown in Fig. 9 (b). In this way, boehmite grew on the CNFs. Consequently, boehmite particles could deposit not only on the disordered inner walls of CNFs but also on the ordered inner walls, as shown in Fig. 4 (e). However, the boehmite that chemically bonded with the CNFs was only boehmite particles reacted with hydrophilic functional groups on the CNFs. And on some sites of the AT5-CNF surfaces, where

hydrophilic functional groups were concentrated as defects, large boehmite particles of about 50 nm in size might deposit, as shown in Fig. 4 (c), (d) and (f). The boehmite on the CNFs was transformed into  $\alpha$ -alumina via transition aluminas with shrinkage by heating. At this time, some alumina particles, particularly those formed on the ordered inner walls of CNFs, fell out of the CNFs, and only those alumina particles which might chemically bond with the CNFs remained on the CNFs.

## 5. Conclusion

We tried to prepare CNFs chemically bonded with alumina particles using acid-treated CNFs and aluminum sec-butoxide. First, the boehmite precursors formed by hydrolysis of aluminum sec-butoxide and the boehmite sols formed by dehydration condensation reactions of the boehmite precursors caused dehydration reactions with hydrophilic functional groups, such as carboxylic (-COOH) and hydroxyl (-OH) groups, modified on the CNFs. If such dehydration reactions actually occur, boehmite chemically bonds with the CNFs. Next, the dehydration condensation reaction was produced again and again between the boehmite formed on the CNFs and boehmite sols in the solution. In this way, boehmite grew on the CNFs. Consequently, boehmite could deposit not only on the disordered inner walls of the CNFs but also on the ordered inner walls. By heating at 1200°C for 1 h under vacuum, the boehmite on the CNFs was transformed into  $\theta$ -alumina and  $\alpha$ -alumina. At this time, some alumina particles, particularly those formed on the ordered inner walls of CNFs, fell out of the CNFs, and only the alumina particles that might chemically bond with the CNFs remained on the CNFs. Finally, the CNFs that were dotted with alumina particles < 50 nm in size were obtained.

## References

- [1] T. Xiao, Y. Ren, K. Liao, P. Wu, F. Li and H. M. Cheng. Determination of tensile strength distribution of nanotubes from testing of nanotube bundles, *Compos. Sci. Technol.* **68** (2008) 2937–42.
- [2] T. Hayashi, Y. A. Kim, T. Natsuki and M. Endo. Mechanical Properties of Carbon Nanomaterials, *ChemPhysChem.* **8** (2007) 999–1004.
- [3] A. H. Barber, I. K. Ashiri, S. R. Cohen, R. Tenne and H. D. Wagner. Stochastic strength of nanotubes: An appraisal of available data, *Compos. Sci. Technol.* **65** (2005) 2380–4.
- [4] C. Wei, K. Cho and D. Srivastava. Tensile strength of carbon nanotubes under realistic temperature and strain rate, *Phys. Rev. B* **67** (2003) 115407.
- [5] M. F. Yu, O. Lourie, M. J. Dyer, K. Moloni, T. F. Kelly and R. S. Ruoff. Strength and Breaking Mechanism of Multiwalled Carbon Nanotubes Under Tensile Load, *Science* **287** (2002) 637–40.
- [6] M. Endo, Y. A. Kim, T. Hayashi, K. Nishimura, T. Matusita, K. Miyashita and M. S. Dresselhaus. Vapor-grown carbon fibers (VGCFs): Basic properties and their battery applications, *Carbon* **39** (2001) 1287–97.
- [7] M. F. Yu, B. S. Files, S. Arepalli and R. S. Ruoff. Tensile Loading of Ropes of Single Wall Carbon Nanotubes and their Mechanical Properties, *Phys. Rev. Lett.* **84** (2000) 5552–5.

- [8] J.P. Salvetat, A.J Kulik, J.M. Bonard, G.A.D. Briggs, T. Stöckli, K. Méténier, S. Bonnamy, F. Béguin, Elastic modulus of ordered and disordered multiwalled carbon nanotubes, *Adv. Matter.* **11** (1999) 161-165.
- [9] N. Ueda, T. Yamakami, T. Yamaguchi, K. Kitajima, Y. Usui, K. Aoki, T. Nakanishi, F. Miyaji, M. Endo, N. Saito and S. Taruta. Fabrication and mechanical properties of high-dispersion-treated carbon nanofiber/alumina composites, *J. Ceram. Soc. Japan* **118** (2010) 847–54.
- [10] N. Ueda, T. Yamakami, T. Yamaguchi, K. Kitajima, Y. Usui, K. Aoki, M. Endo, N. Saito and S. Taruta. Microstructure development and fracture toughness of acid-treated carbon nanofibers/alumina composites, *J. Ceram. Soc. Japan* **120** (2012) 560–8.
- [11] N. Ueda, T. Yamakami, T. Yamaguchi, Y. Usui, K. Aoki, M. Endo, N. Saito and S. Taruta. Influence of CNF content on microstructure and fracture toughness of CNF/alumina composites, *J. Ceram. Soc. Japan* **122** (2014) 292–9.
- [12] K. Hernadi, E. Ljubović, J. W. Soe and L. Forró. Synthesis of MWNT-based composite materials with inorganic coating, *Acta Mater.* **51** (2003) 1447-52.
- [13] K. Hernadi, E. Couteau, J.W. Soe, L. Forró. Al(OH)<sub>3</sub>/multiwalled carbon nanotube composite: homogeneous coverage of Al(OH)<sub>3</sub> on carbon nanotube surfaces, *Langmuir* **19** (2003) 7026-7029.
- [14] Q. Yang, Y. Deng and W. Hu. Preparation of alumina/carbon nanotubes composites

- by chemical precipitation, *Ceram. Int.* **35** (2009) 1305-10.
- [15] G. Yamamoto, M. Omori, T. Hashida and H. Kimura. A novel structure for carbon nanotube reinforced alumina composites with improved mechanical properties, *Nanotechnology* **19** (2008) 215708 (7 pp).
- [16] F. Avilés, J.V. Cauich-Rodríguez, L. Moo-Tah, A. May-Pat, R. Vargas-Coronado, Evaluation of mild acid oxidation treatments for MWCNT functionalization, *Carbon* **47** (2009) 2970–2975.
- [17] P.-X. Hou, C. Liu and H.-M. Cheng. Purification of carbon nanotubes, *Carbon* **46** (2008) 2003-25.
- [18] I. Levin and D. Brandon. Metastable alumina polymorphs: crystal structures and transition sequences, *J. Am. Ceram. Soc.* **81** (1998) 1995-2012.

## Figure Captions

**Fig. 1** TEM images of (a and b) pristine CNFs and (c and d) AT5-CNFs. (a and c) low magnification; (b and d) high magnification

**Fig. 2** XRD patterns of alumina precursor-deposited (a) AT05-CNFs and (b) AT5-CNFs

**Fig. 3** FE-SEM images of boehmite-deposited (a and b) AT05-CNFs and (c and d) AT5-CNFs. (a and c) low magnification; (b and d) high magnification

**Fig. 4** TEM images of boehmite-deposited (a and b) AT05-CNFs and (c, d, e and f) AT5-CNFs. (a and c) low magnification; (b, d, e and f) high magnification

**Fig. 5** XRD patterns of boehmite-deposited (a) AT05-CNFs and (b) AT5-CNFs after heating at 1200°C for 1 h under vacuum

**Fig. 6** FE-SEM images of alumina-deposited (a) AT05-CNFs and (b) AT5-CNFs

**Fig. 7** TEM images of alumina-deposited (a) AT05-CNFs and (b) AT5-CNFs

**Fig. 8** Raman spectra of AT05-CNFs, boehmite-deposited AT05-CNFs, and alumina-deposited AT05-CNFs

**Fig. 9** Schematic illustration of forming processes of  $\alpha$ -alumina particles on CNFs. (a) dehydration reactions between boehmite precursors (or boehmite sols) and hydrophilic functional groups on CNFs; (b) dehydration condensation reactions between boehmite particles formed on CNF and boehmite sols; (c) transformation of boehmite particles on CNFs into  $\alpha$ -alumina particles by heating at 1200°C under vacuum

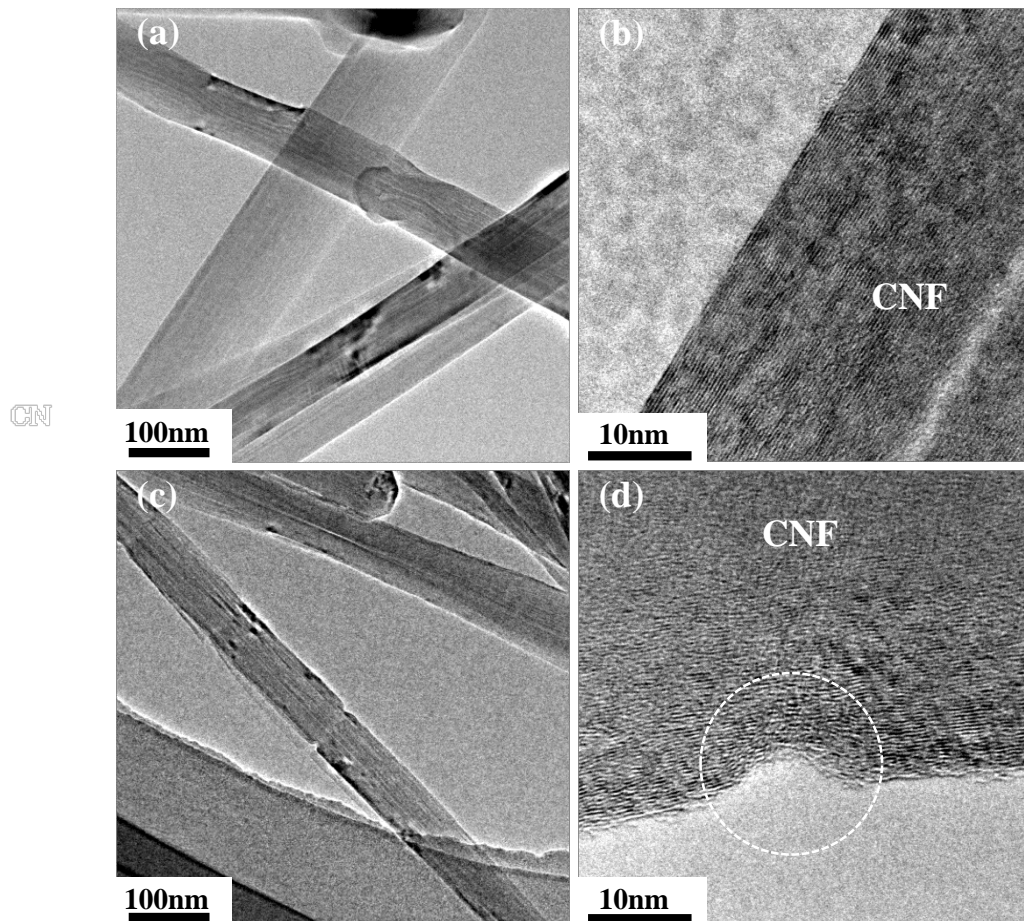


**Fig. 1** TEM images of (a and b) pristine CNFs and (c and d) AT5-CNFs. (a and c) low magnification; (b and d) high magnification

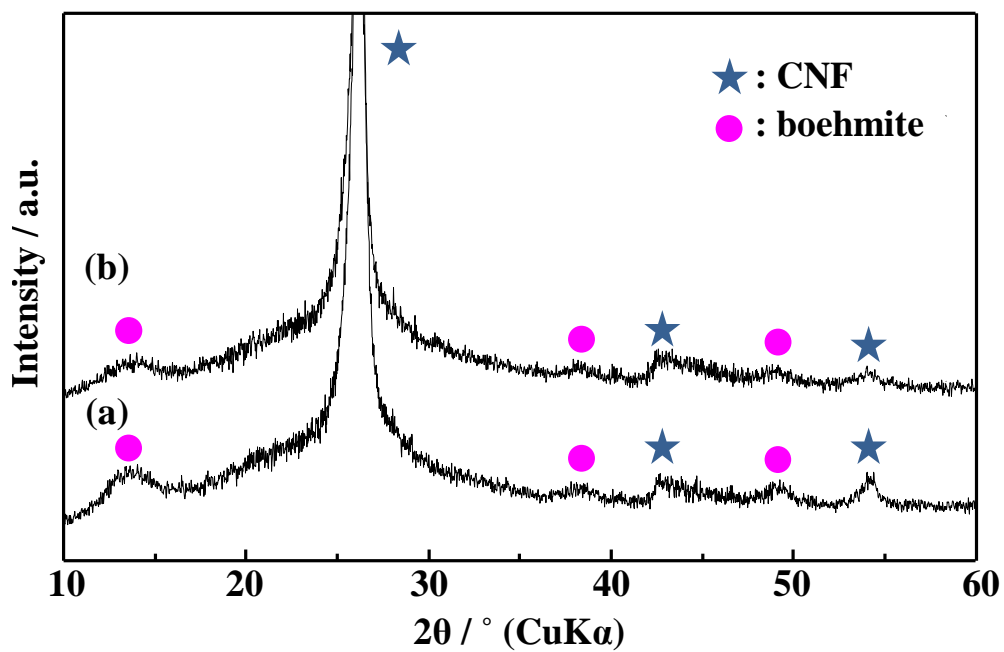


**Fig. 2** XRD patterns of alumina precursor-deposited (a) AT05-CNFs and (b) AT5-CNFs

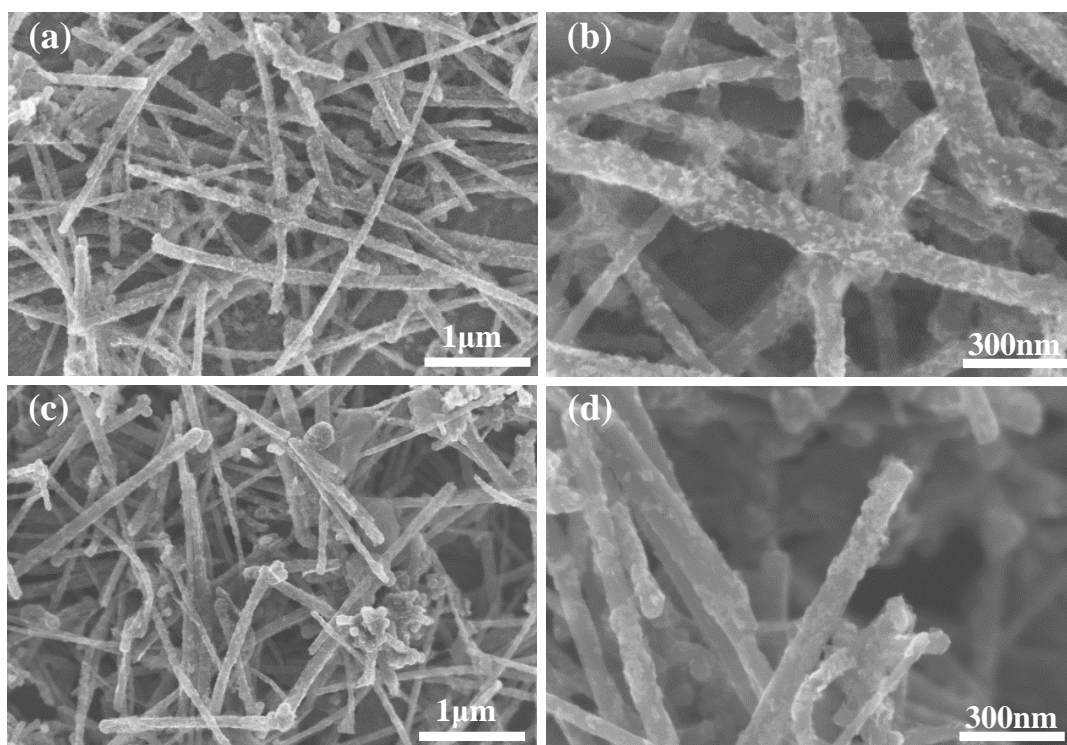


**Fig. 3** FE-SEM images of boehmite-deposited (a and b) AT05-CNFs and (c and d) AT5-CNFs. (a and c) low magnification; (b and d) high magnification

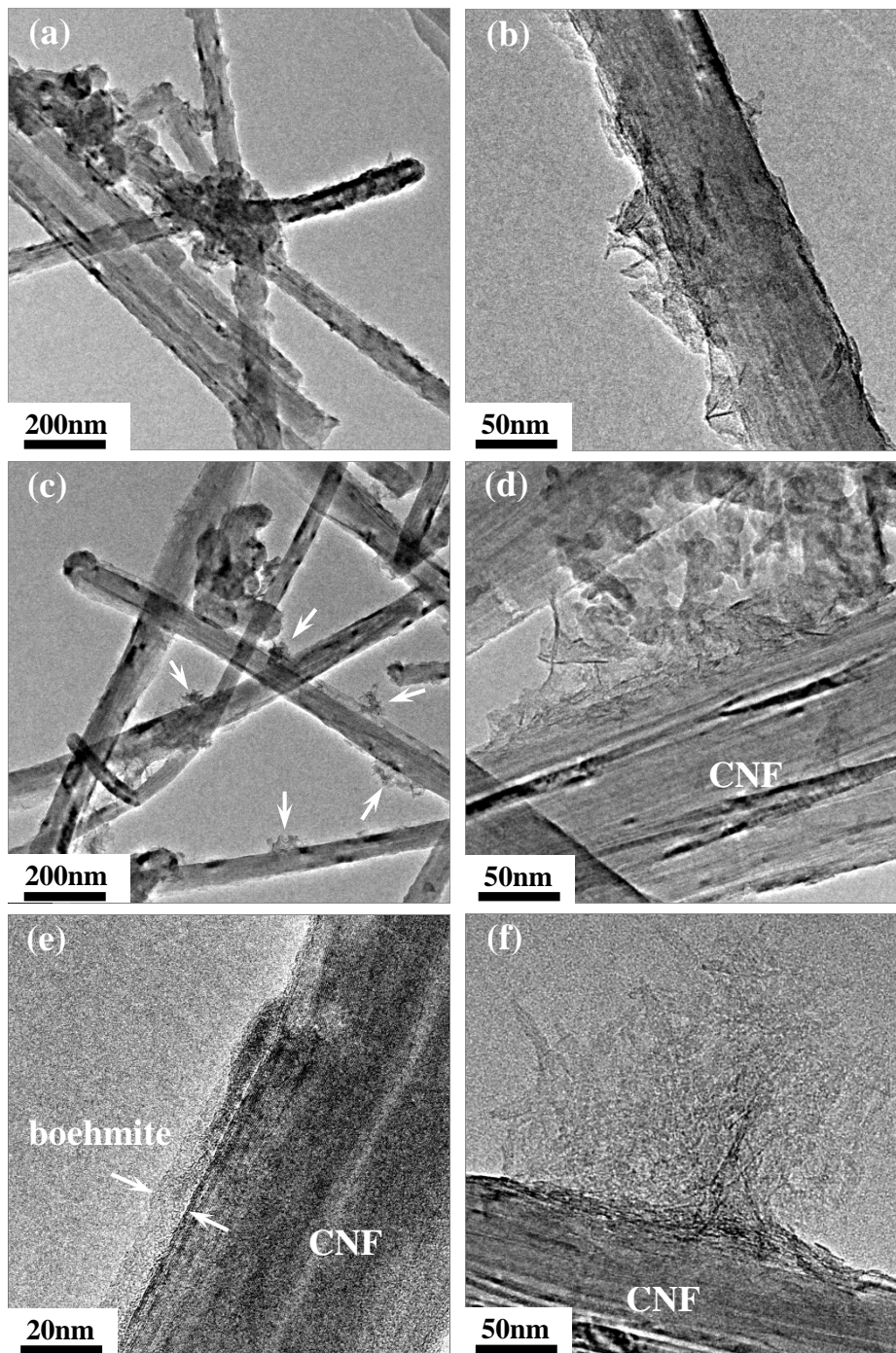


**Fig. 4** TEM images of boehmite-deposited (a and b) AT05-CNFs and (c, d, e and f) AT5-CNFs. (a and c) low magnification; (b, d, e and f) high magnification

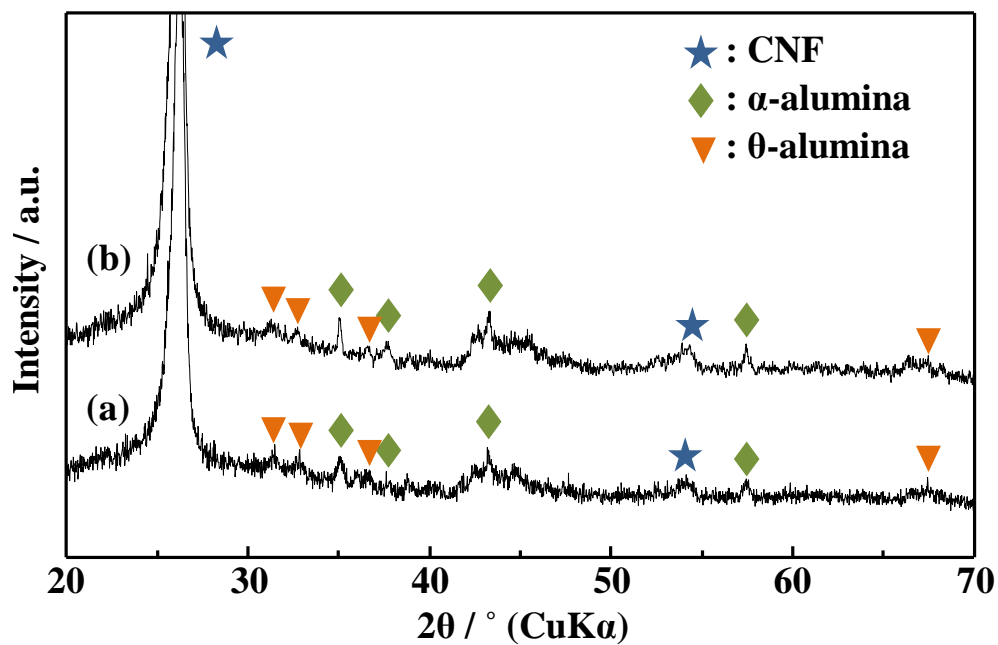


**Fig. 5** XRD patterns of boehmite-deposited (a) AT05-CNFs and (b) AT5-CNFs after heating at  $1200^\circ\text{C}$  for 1 h under vacuum

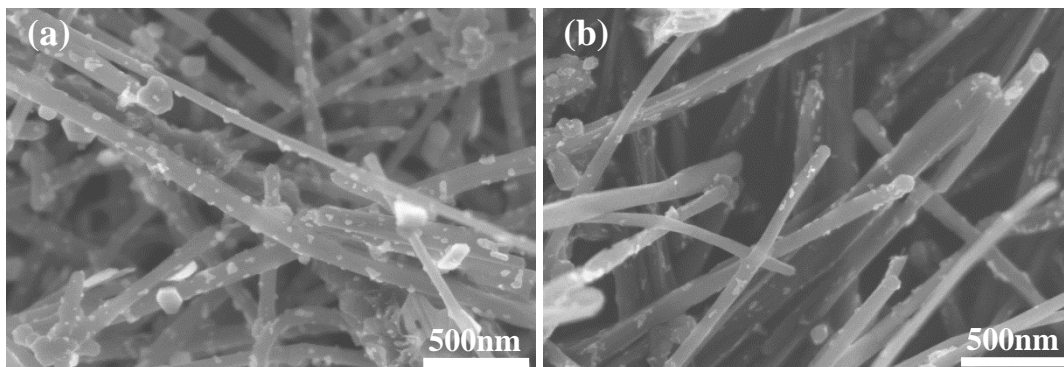


**Fig. 6** FE-SEM images of alumina-deposited (a) AT05-CNFs and (b) AT5-CNFs

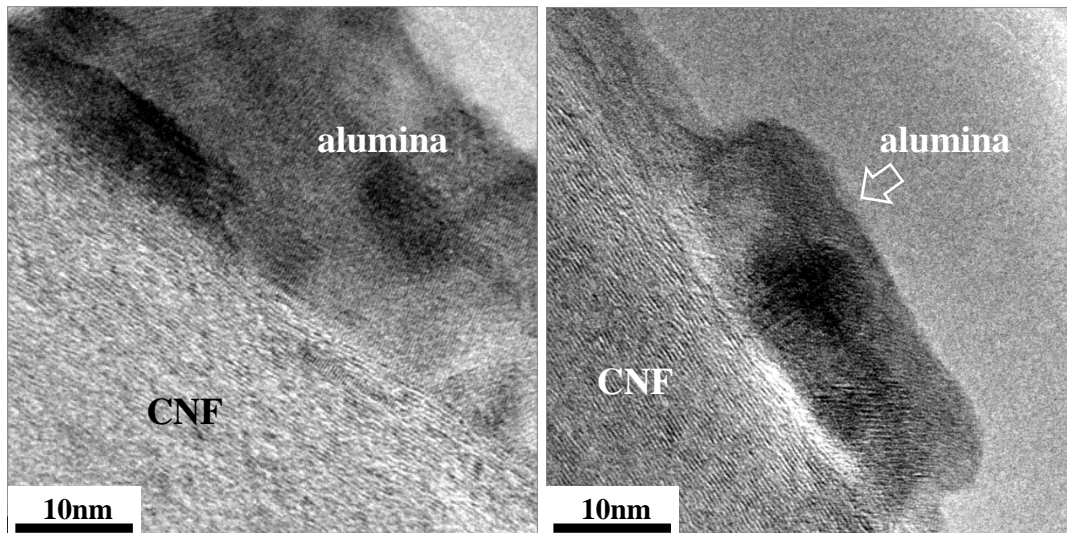


**Fig. 7** TEM images of alumina-deposited (a) AT05-CNFs and (b) AT5-CNFs

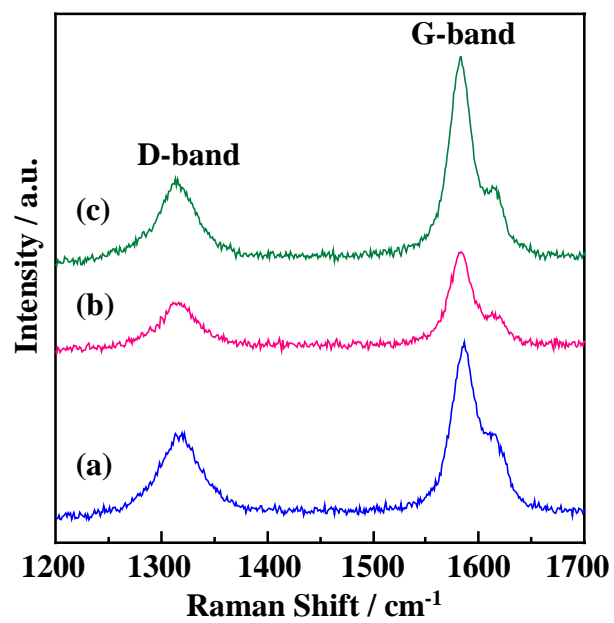


**Fig. 8** Raman spectra of AT05-CNFs, boehmite-deposited AT05-CNFs, and alumina-deposited AT05-CNFs

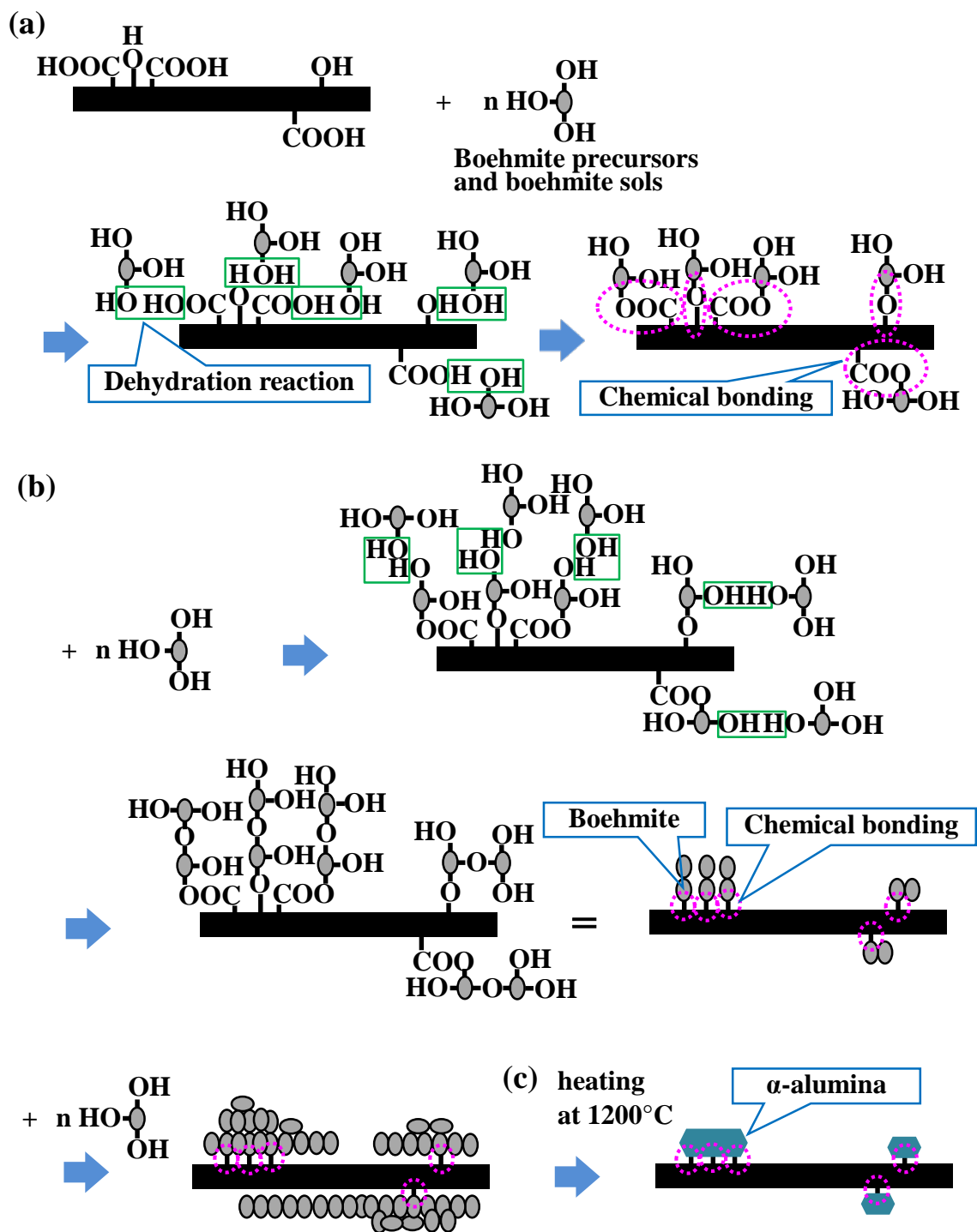


**Fig. 9** Schematic illustration of forming processes of  $\alpha$ -alumina particles on CNFs. (a) dehydration reactions between boehmite precursors (or boehmite sols) and hydrophilic functional groups on CNFs; (b) dehydration condensation reactions between boehmite particles formed on CNF and boehmite sols; (c) transformation of boehmite particles on CNFs into  $\alpha$ -alumina particles by heating at 1200°C under vacuum